

Exact solution to simultaneous intensity and phase encryption with a single phase-only hologram

Eliot Bolduc,¹ Nicolas Bent,¹ Enrico Santamato,² Ebrahim Karimi,^{1,*} and Robert W. Boyd^{1,3}

¹Department of Physics, University of Ottawa, 150 Louis Pasteur, Ottawa, Ontario K1N 6N5, Canada

²Dipartimento di Scienze Fisiche, Università di Napoli "Federico II", Complesso di Monte S. Angelo, 80126 Napoli, Italy

³Institute of Optics, University of Rochester, Rochester, New York 14627, USA

*Corresponding author: ekarimi@uottawa.ca

Received July 19, 2013; revised August 12, 2013; accepted August 13, 2013;
posted August 14, 2013 (Doc. ID 194221); published September 5, 2013

A phase-only hologram applies a modal transformation to an optical transverse spatial mode via phase encoding and intensity masking. Accurate control of the optical field crucially depends on the method employed to encode the hologram. In this Letter, we present a method to encode the amplitude and the phase of an optical field into a phase-only hologram, which allows the exact control of spatial transverse modes. Any intensity masking method modulates the amplitude and alters the phase of the optical field. Our method consists in correcting for this unwanted phase alteration by modifying the phase encryption accordingly. We experimentally verify the accuracy of our method by applying it to the generation and detection of transverse spatial modes in mutually unbiased bases of dimension two and three. © 2013 Optical Society of America

OCIS codes: (090.1760) Computer holography; (100.5090) Phase-only filters; (070.2580) Paraxial wave optics; (260.6042) Singular optics; (270.5568) Quantum cryptography.

<http://dx.doi.org/10.1364/OL.38.003546>

The generation of optical fields possessing specific transverse intensity and phase distributions is highly important in many different research areas such as stimulated emission depletion microscopy, optical trapping, optical tweezers, communication, data storage, and fundamental quantum mechanics [1–5]. Nowadays, technologies such as spatial light modulators (SLMs) and assorted controllable micromirrors provide an easy way to generate and manipulate optical fields from computer generated phase-only holograms, otherwise called holographic kinoforms [6,7]. Generating an arbitrary beam accurately requires engineering both phase and amplitude structures simultaneously. The current available devices are fabricated to physically control only the phase or amplitude of an optical field, but not both at the same time. Combining these two devices together allows one to control both the phase and amplitude of an optical field. However, there exists techniques to modulate both properties simultaneously with a single device [8].

Over the course of the last five decades, many intensity-masking methods for holographic kinoforms were proposed by many different groups [9–12]. All these techniques make use of a grating pattern whose diffraction efficiency is modulated by a function of the amplitude of the beam. Indeed, intensity masking, i.e., encrypting an arbitrary function of the amplitude onto a holographic kinoform, is a selective process that diffracts only the desired part of the incoming beam into the first order of diffraction and the undesired part, depending on the techniques, remains in the zero order, diffracts into higher orders or both. The diffraction efficiency depends on the depth of phase of the blazing in the grating pattern; the closer to a full-phase, i.e., 2π , variation in the blazing, the more light diffracts [10]. Such a phase modulation gives the ability to control the diffracted intensity as a function of the transverse coordinates and thus allows

one to generate or transform any transverse spatial mode within the capabilities of the device.

Recently, Ando *et al.* numerically compared the purity of the generated mode of different intensity masking methods [13]. These methods can yield good approximations to the desired mode transformation, but an exact solution was yet to be found. In this Letter, we present the exact solution to the necessary phase encoding and intensity masking on a phase-only hologram for any given paraxial mode transformation. We experimentally put our technique to the test by generating and detecting orbital angular momentum (OAM) states of light with two SLMs. We choose OAM subspaces of two and three dimensions and consider the states in all mutually unbiased bases (MUBs), which consists of both eigenstates and superposition states.

In solving the problem of encryption of a holographic kinoform, we use a plane wave as the incident optical field, and define the desired output beam as the following scalar paraxial field:

$$E(\mathbf{r}_\perp, z_0) := A(\mathbf{r}_\perp, z_0) e^{i\Phi(\mathbf{r}_\perp, z_0)}, \quad (1)$$

where \mathbf{r}_\perp stands for the transverse coordinate, $A(\mathbf{r}_\perp, z_0) := |E(\mathbf{r}_\perp, z_0)|$ and $\Phi(\mathbf{r}_\perp, z_0) := \text{Arg}(E(\mathbf{r}_\perp, z_0))$ are the amplitude and phase of the optical field at the $z = z_0$ plane, respectively. As Eq. (1) suggests, a scalar optical field is well-defined in the entire space by two independent real functions, one specifying the amplitude profile and the other specifying the phase distribution. This is fundamentally governed by the angular spectrum method, which defines the optical field at any given z plane uniquely if the initial pupil field function is given. In our derivations, we specify A and Φ in the plane of the hologram ($z = 0$).

Let us first consider the simple case of a holographic kinoform with no intensity masking and an imprinted phase profile of $\Psi(m, n) = \text{Mod}(\Phi(m, n) + 2\pi m/\Lambda, 2\pi)$, where m and n are the pixel coordinates and Λ is the period of the blazed grating pattern—the type of grating that maximizes the diffraction efficiency. A Fourier analysis shows that, in the limit of infinitely many pixels, the optical field in the first order of diffraction is simply given by $\vec{E}_{\text{out}} = \text{FT}[\exp(i\Phi(m, n))]$, where FT corresponds to the Fourier transform. To express the output beam in the near-field of the hologram, the standard procedure is to insert a spatial filter that selects only the first diffracted order and go to the Fourier plane of the spatial filter. The output beam in the near-field of the hologram is then written $E_{\text{out}} = \exp(i\Phi(m, n))$. The encrypted phase profile $\Phi(m, n)$ is directly transferred to the output optical field, whose amplitude stays uniform. In the following section, we show how to simultaneously obtain the exact desired amplitude and phase profiles in the image plane, or near-field, of a hologram.

We now consider a very general case of simultaneous phase and amplitude encoding of a phase-only hologram. The imprinted phase profile on the hologram is given by $\Psi(m, n) = \mathcal{M}(m, n)\text{Mod}(\mathcal{F}(m, n) + 2\pi m/\Lambda, 2\pi)$, where \mathcal{M} is a normalized bounded positive function of amplitude, i.e., $0 \leq \mathcal{M} \leq 1$, and \mathcal{F} is an analytical function of the amplitude and phase profiles of the desired field. Just after passing through the hologram, the input plane wave acquires the imprinted phase profile and is given by

$$T(m, n) = e^{i\mathcal{M}(m, n)\text{Mod}(\mathcal{F}(m, n) + 2\pi m/\Lambda, 2\pi)}. \quad (2)$$

A calculation based on a Taylor–Fourier expansion shows that the action of this particular optical phase object—after spatial filtering of all orders except the first one—can be expressed as

$$T_1(m, n) = -\text{sinc}(\pi\mathcal{M} - \pi)e^{i(\mathcal{F} + \pi\mathcal{M})}, \quad (3)$$

where \mathcal{M} and \mathcal{F} are both functions of the transverse coordinates on the hologram, i.e., $\{m, n\}$ [10]. Since the output mode must be exactly equal to the desired field of Eq. (1), we find that the two modulation functions are given by

$$\begin{aligned} \mathcal{M} &= 1 + \frac{1}{\pi} \text{sinc}^{-1}(A) \\ \mathcal{F} &= \Phi - \pi\mathcal{M}, \end{aligned} \quad (4)$$

where $\text{sinc}^{-1}(\cdot)$ stands for the inverse function of the sinc, and $\text{sinc}(x) = \sin x/x$ is an unnormalized sinc function in the domain of $[-\pi, 0]$, which accounts for the minus sign in Eq. (3). The form of the intensity modulation function \mathcal{M} is such that there is a linear relationship between the desired amplitude and the encoded amplitude, see solid red curve in Fig. 1. Moreover, we cancel the unwanted phase $\pi\mathcal{M}$ in Eq. (3) by subtracting it in the phase encoding function \mathcal{F} . Crucially, Eq. (4) decouples the generated phase profile from the two-dimensional amplitude distribution. Replacing the terms of Eq. (4) into $\Psi(m, n)$, the imprinted phase profile on the

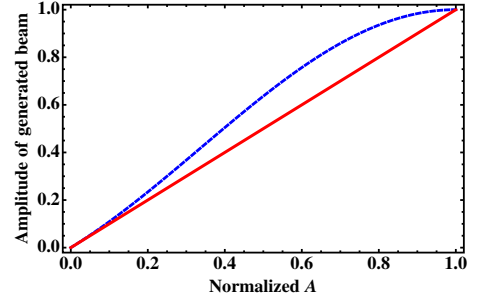


Fig. 1. Amplitude of the generated beam, after selection of the first order of diffraction, as a function of the normalized desired amplitude of Eq. (1). The solid-red curve corresponds to our exact hologram encryption method; the generated amplitude is equal to the desired amplitude. The blue dashed curve is based on the technique reported in [10].

hologram, completes the description of our method. Since this result is exact, the fidelity of the generated modes should now only be limited by the capabilities of the device it is used with.

In order to test for the ability to encode and decode information on transverse spatial modes, we experimentally applied our method to the generation and detection of states in MUBs. Eigenstates of $\{|u_i\rangle\}$ and $\{|v_j\rangle\}$ are called MUBs in the Hilbert space of dimension d if $|\langle u_i | v_j \rangle|^2 = 1/d$ for any i and j . For a given generated mode, we perform a complete set of projections, whose outcomes allow us to determine the generated mode. The process of reconstructing a state from a complete set of measurement outcomes is known as quantum state tomography. This test is experimentally very reliable, and it is exhaustive, since it requires the generation and detection of all informationally independent eigenstates and superposition states.

Without loss of generality and only for this test, we neglect the radial dependence of the optical field, and we consider only the azimuthal part associated with optical OAM. An optical beam with an azimuthal phase profile of the form $\exp(i\ell\phi)$ carries a well-defined OAM value of $\ell\hbar$ per photon, where ϕ is the cylindrical coordinate. These beams are eigenstates of the z -component of the OAM operator and form a complete basis in the azimuthal coordinate, $\langle \mathbf{r} | \ell \rangle = \exp(i\ell\phi)$ [5].

MUBs form a complete set of bases. For a Hilbert space of dimension d equal to a prime or the power of a prime, the total number of MUBs is known to be $d + 1$ [14]. In the $d = 2$ OAM Hilbert subspace, the $(2 + 1)$ MUBs are eigenstates of the Pauli matrices. In analogy with polarization, this state space can be mapped on an OAM Poincaré sphere [15]. The set of MUBs in two-dimensional Hilbert space are given by

$$\begin{aligned} \{\text{I}\} &= \{|0\rangle, |1\rangle\} \\ \{\text{II}\} &= \left\{ \frac{|0\rangle + |1\rangle}{\sqrt{2}}, \frac{|0\rangle - |1\rangle}{\sqrt{2}} \right\} \\ \{\text{III}\} &= \left\{ \frac{|0\rangle + i|1\rangle}{\sqrt{2}}, \frac{|0\rangle - i|1\rangle}{\sqrt{2}} \right\}. \end{aligned} \quad (5)$$

For a three-dimensional OAM Hilbert subspace, the $(3 + 1)$ MUBs are given by

$$\begin{aligned}
\{\text{I}\} &= \{|0\rangle, |1\rangle, |2\rangle\} \\
\{\text{II}\} &= \left\{ \frac{|0\rangle + |1\rangle + |2\rangle}{\sqrt{3}}, \frac{|0\rangle + \omega|1\rangle + \omega^2|2\rangle}{\sqrt{3}}, \frac{|0\rangle + \omega^2|1\rangle + \omega|2\rangle}{\sqrt{3}} \right\} \\
\{\text{III}\} &= \left\{ \frac{|0\rangle + \omega|1\rangle + \omega^2|2\rangle}{\sqrt{3}}, \frac{|0\rangle + \omega^2|1\rangle + |2\rangle}{\sqrt{3}}, \frac{|0\rangle + |1\rangle + \omega^2|2\rangle}{\sqrt{3}} \right\} \\
\{\text{IV}\} &= \left\{ \frac{|0\rangle + \omega^2|1\rangle + \omega^2|2\rangle}{\sqrt{3}}, \frac{|0\rangle + \omega|1\rangle + |2\rangle}{\sqrt{3}}, \frac{|0\rangle + |1\rangle + \omega|2\rangle}{\sqrt{3}} \right\},
\end{aligned} \tag{6}$$

where $\omega = \exp(i2\pi/3)$ [16,17].

We implement our method in computer-generated holograms displayed on cost-effective Cambridge Correlators SLMs, with a resolution of 1024×786 pixels. A layout of the experimental setup used to perform the MUB test is shown in Fig. 2. A 3 mm wide single-mode HeNe laser beam goes through a polarizer that optimizes the diffraction efficiency of SLM-A. This SLM transforms the input flat-phase field into any of the states given in Eqs. (5) and (6). The beam then traverses a spatial filter that selects out all but the first order of diffraction. The half-wave plate modifies the polarization to optimize the diffraction efficiency of SLM-B, which applies a second modal transformation to the laser beam. Together with the single-mode fiber (SMF) and an iris, SLM-B projects the generated mode onto an arbitrary mode in Eqs. (5) and (6). We measure the strength of the projections with a power-meter at the output of the SMF. In other words, SLM-A forms the state and SLM-B and SMF together analyze the state.

Because of the fact that we use intensity masking, we have to normalize each projective measurement by the reflection efficiencies of the displayed holograms on each SLM. For example, when displaying an OAM eigenstate on SLM-A, no intensity masking is needed because we ignore the radial degree of freedom and it has a flat azimuthal intensity distribution. However, a

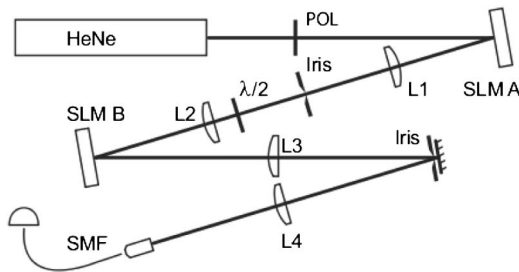


Fig. 2. Layout of the experimental setup used to encode and detect OAM qubit and qutrit states based on our new method. A HeNe laser beam illuminates SLM-A, which generates any of the MUBs. The $4f$ systems made of the lenses $\{L1, L2\}$ image the plane of SLM-A to that of SLM-B with unit magnification. The SLM-B and a SMF act together as a mode projector on any of the MUBs states. We sequentially display all MUBs states on SLM-A and SLM-B, and acquire all combinations of projections. The last set of lenses, composed of $\{L3, L4$, microscope objective $\}$, take the far-field of SLM-B to the entrance facet of the SMF. The irises act as spatial filters which select the first order of diffraction of SLM-A and SLM-B. As SLMs are polarization sensitive, the polarizer (POL) and the half-wave plate ($\lambda/2$) optimize the diffraction efficiency.

superposition state, a so-called *angle* state, requires intensity masking since the azimuthal symmetry is broken. In dimension two, half of the light will be lost. We have to take this mode-dependent reflection efficiency into account. Thus, for each hologram displayed on SLM-A and SLM-B, we measure the power of the reflected light in the first order of diffraction of each SLM, and normalize the projection outcomes by the reflection efficiencies of each SLM. Figure 3 shows the normalized outcomes of the projections for $d = 2$ and $d = 3$ OAM Hilbert subspaces. We measure the quality of the system with a figure of merit called *similarity* S [18], an analogous quantity to the fidelity in the case of pair of states. Our system yields similarities of $S = 0.993$ and $S = 0.927$ for dimension two and three, respectively.

Our method requires the calculation of the inverse sinc function for every pixel on the hologram, and this task can be computationally intensive for a standard computer. For simplicity and speed, it is sometimes more convenient to implement a hologram encryption method that only requires standard functions, unlike the inverse sinc function. We thus propose a simple improvement over the already simple technique first reported by Davis *et al.* [10]. In the case where the intensity modulation function is given by $\mathcal{M} = A$ and $\mathcal{F} = \Phi$, as proposed by Davis *et al.*, the optical transverse mode after spatial filtering is equal to $\text{sinc}(\pi(A - 1)) \exp(i(\Phi + \pi A))$ in the near-field of the hologram. For this method, the amplitude profile of the generated beam $\text{sinc}(\pi(A - 1))$ is always rather close to that of the desired amplitude A [see dashed blue curve in Fig. 1]. In fact, the normalized generated and desired amplitudes are never further apart than 0.161, $|\text{sinc}(\pi(A - 1)) - A| < 0.161$. The difference in amplitude distributions is not as significant as the difference in phase profiles. The generated phase profile can be completely modified by the supplementary term πA in the exponential. We thus propose a simple improvement that consists in modifying the phase encryption \mathcal{F} as in Eq. (4): $\mathcal{F} = \Phi - \pi A$. In principle, this new method does not yield an exact replica of the desired field since it does not correct for the gap in amplitude, but it should give good approximations because it solves the problem of the extra phase term, which is much more important.

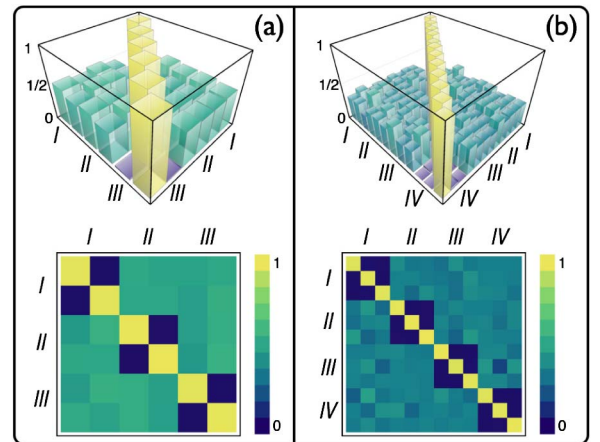


Fig. 3. Experimental projections between states in all MUBs in (a) $d = 2$ and (b) $d = 3$ OAM Hilbert subspaces, i.e., $P_{ij} = |\langle \alpha_i | \beta_j \rangle|^2$.

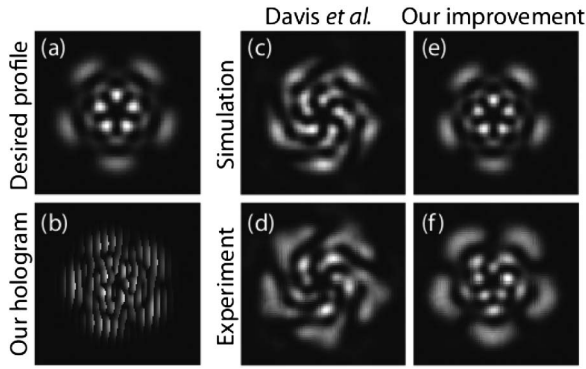


Fig. 4. Qualitative comparison of the method of Davis *et al.* and our proposed improvement of their technique. The desired intensity profile purposely has small features to accentuate the difference between the two methods. The experimentally recorded images are taken in the far-field of a HOLOEYE SLM.

Just like the original method of Davis *et al.*, it has the advantage of being very easy to implement. Note that the proposed method in [10] aimed to encode the *amplitude* of an optical field and not the phase.

We experimentally compare the method of Davis *et al.* with our proposed improvement by recording the intensity profiles of a transverse mode generated with each technique. The desired intensity profiles is that of a superposition of two Laguerre–Gaussian (LG) modes, $LG_2^{-2} + LG_1^3$, where LG_p^ℓ is the LG mode with the radial and azimuthal indices of p and ℓ , respectively. Figure 4 shows the results of a numerical simulation with each method and the experimentally recorded intensity profiles, respectively. Although this comparison is only qualitative, the difference between the intensity profiles of the generated output modes is striking.

In conclusion, we have presented a new way of encoding the amplitude and the phase of an optical field into a pure-phase hologram. The encryption is based on intensity masking, whereby the amplitude distribution of a desired optical field modulates the profile of the encoded phase. In order to measure the accuracy of the method, we performed a complete test over all informationally independent OAM states in the subspaces of dimension two and three, the results of which are in excellent agreement with theory. This result suggests that our method allows the generation of arbitrary transverse spatial modes with high accuracy. We also proposed a simple improvement of the easy-to-implement method of Davis *et al.* A qualitative comparison of the intensity

distribution of a mode with small features showed that the improvement is highly significant. We thus showed a very simple way of encoding phase-only holograms for the purpose of generating high fidelity spatial transverse modes.

E. B., N. B., E. K., and R. W. B. acknowledge the support of the Canada Excellence Research Chairs (CERC) Program. E. B. acknowledges the financial support of the FQRNT, grant number 149713. E. S. acknowledges the financial support of the Future and Emerging Technologies (FET) programme within the Seventh Framework Programme for Research of the European Commission, under FET-Open grant number 255914-PHORBITECH.

References and Note

1. W. S. Hell, *Science* **316**, 1153 (2007).
2. H. He, N. R. Heckenberg, and H. Rubinsztein-Dunlop, *J. Mod. Opt.* **42**, 217 (1995).
3. L. Paterson, M. P. MacDonald, J. Arlt, W. Sibbett, P. E. Bryant, and K. Dholakia, *Science* **292**, 912 (2001).
4. G. Gibson, J. Courtial, M. J. Padgett, M. Vasnetsov, V. Pasko, S. M. Barnett, and S. Franke-Arnold, *Opt. Express* **12**, 5448 (2004).
5. S. Franke-Arnold, L. Allen, and M. Padgett, *Laser Photon. Rev.* **2**, 299 (2008).
6. J. A. Neff, R. A. Athale, and S. H. Lee, *Proc. IEEE* **78**, 826 (1990).
7. V. Yu. Bazhenov, M. S. Soskin, and M. V. Vasnetsov, *J. Mod. Opt.* **39**, 985 (1992).
8. V. A. Soifer, eds., *Methods for Computer Design of Diffractive Optical Elements* (Wiley, 2002).
9. J. P. Kirk and A. L. Jones, *J. Opt. Soc. Am.* **61**, 1023 (1971).
10. J. A. Davis, D. M. Cottrell, J. Campos, M. J. Yzuel, and I. Moreno, *Appl. Opt.* **38**, 5004 (1999).
11. J. Leach, M. R. Dennis, J. Courtial, and M. J. Padgett, *New J. Phys.* **7**, 55 (2005).
12. V. Arrizón, U. Ruiz, R. Carrada, and L. A. González, *J. Opt. Soc. Am. A* **24**, 3500 (2007).
13. T. Ando, Y. Ohtake, N. Matsumoto, T. Inoue, and N. Fukuchi, *Opt. Lett.* **34**, 34 (2009).
14. W. K. Wootters and B. D. Fields, *Ann. Phys.* **191**, 363 (1989).
15. M. J. Padgett and J. Courtial, *Opt. Lett.* **24**, 430 (1999).
16. M. Wieśniak, T. Paterek, and A. Zeilinger, *New J. Phys.* **13**, 053047 (2011).
17. V. D'Ambrosio, F. Cardano, E. Karimi, E. Nagali, E. Santamato, L. Marrucci, and F. Sciarrino, arXiv:1304.4081.
18. The similarity is defined as $S = \left(\frac{\left(\sum_{i,j} \sqrt{P_{ij}P'_{ij}} \right)^2}{\sum_{i,j} P_{ij} \sum_{i,j} P'_{ij}} \right)$, where P and P' stand for experimental and expected theoretical projection matrix.